This article appeared in J. Mater. Chem. C, 2023, 11, 10266-10273, DOI:10.1039/D3TC00734K and may be found at https://pubs.rsc.org/en/content/articlelanding/2023/tc/d3tc00734k

Modulation of charge transfer exciton dynamics in organic semiconductors using different structural arrangements

Cristian Soncini, Abhishek Kumar, Federica Bondino, Elena Magnano, Matija Stupar, Barbara Ressel, Giovanni De Ninno, Antonis Papadopoulos, Efthymis Serpetzoglou, Emmanuel Stratakis and Maddalena Pedio, *J. Mater. Chem. C*, 2023, **11**, 10266-10273, **DOI:**10.1039/D3TC00734K

Received 00th January 20xx,
Accepted 00th January 20xx

DOI:

Modulation of Charge Transfer Exciton Dynamics in Organic Semiconductors Using Different Structural Arrangements

Cristian Soncini,[a] Abhishek Kumar,[b] Federica Bondino,[a] Elena Magnano,[a,c] Matija Stupar,[d†] Barbara Ressel,[d] Giovanni De Ninno,[d,e] Antonis Papadopoulos,[f] Efthymis Serpetzoglou,[f] Emmanuel Stratakis,[f] and Maddalena Pedio[a]*

In devices based on organic semiconductors, aggregation and inter-molecular interactions play a key role in affecting the photo-physical and dynamical carrier properties of the material, potentially becoming a limiting factor to achieving high efficiency. As a consequence, a detailed understanding of the interplay between the film molecular structure and the material properties is essential to properly design devices with optimized performance. Here we demonstrate how different molecular structural arrangements modulate the charge transfer (CT) dynamics in cobalt phthalocyanine (CoPc) thin films. By transient absorption spectroscopy and time-resolved photoemission spectroscopy, we study the influence of different CoPc structures on the dynamical electronic properties, the CoPc intra and inter-molecular de-excitation pathways up to 7 ns. We rationalize the ultrafast formation of triplet states in the CoPc through an electron exchange process between the single-occupied Co3d$_{z^2}$ orbital and π orbitals of the macrocycle, which obviate for an energetically unfavourable spin-flip. We found enhanced CT exciton lifetime in the case of the herringbone structure with respect to the brickstone one, possibly explainable by a more efficient CT exciton delocalization along the stacking axis.

1 Introduction

Charge transfer (CT) processes in organic semiconductors play a key role in several physical phenomena and technological applications, including electron transport, solar cells, organic light-emitting devices and spintronics[1-4]. One critical issue to overcome toward highly-efficient devices is the need for a deeper understanding of the fundamental factors that influence the CT process to achieve thorough control at the nanoscale. In this framework, the CT in conjugated systems is strongly related to the optimal overlap of the π orbitals along the direction of carrier flow[3-5]. Therefore, molecules with rigid and planar π systems which self-assemble in long-range columnar structures exhibit great potential in achieving enhanced charge transport properties[6-7]. In recent years, many studies pointed out the active role of the aggregation and inter-molecular interactions in tuning the photo-physical and dynamical carrier properties of the film, affecting the light absorption, the energy level alignment, the exciton diffusion, allowing for more efficient charge transport in the material[6-11]. As a consequence, accurate control of the molecular structure in the solid aggregation is a key factor in designing and optimizing the device performance, implying the possibility of ad-hoc engineering of the electronic properties and the carrier transport dynamics in molecular films. Here we demonstrate how different molecular structural arrangements modulate the CT exciton dynamic in ordered cobalt phthalocyanine (CoPc) thin films. The CoPc represents a case system of particular interest since, in the solid state, forms π-conjugated structures with significant structural anisotropy along the stacking axis. Substantial anisotropy may therefore exist in the CT exciton delocalization in CoPc films. As a case in point, Gadalla and co-workers reported the possibility of a preferential CT exciton energy transfer along the CoPc stacking axis due to a band of CT exciton states[12]. They suggest that such CT states band may be originated from the strong coupling between adjacent CoPc molecules (along the stacking axis) induced by the single-occupied out-of-plane Co3d$_{z^2}$ orbital. The substantial impact of the Co3d$_{z^2}$ orbital in the molecular dynamics can be understood simply by comparing the transient absorption spectroscopy (TAS) studies on α-CoPc and α-copper phthalocyanine (CuPc) films of ref. 12 and ref. 13, respectively (we recall that in the CuPc the single-occupied metal orbital is the 3d$_{x^2-y^2}$ - in-plane oriented). The TAS spectra show different evolution in time of the singlet excited states, decaying in a few of ps in the CoPc[12] and hundreds of ps in the CuPc[13]. Furthermore, the CoPc spectra show an additional excited state absorption (ESA) feature directly related to the formation of triplet states[12]. Such differences suggest a possible important contribution of the Co3d$_{z^2}$ in modifying as well as providing additional relaxation channels to the excited states. For these reasons, we used a multi-technique approach to get a deeper understanding of how the molecular stacking geometry and the Co3d$_{z^2}$ orbital influence the CoPc dynamical electronic properties. In this regard, the optimization of the intermolecular interactions to promote an efficient orbital overlap between adjacent planes is strongly determined by the molecular stacking geometry in the film (stacking angle, sliding angle and Co-Co inter-plane distance)[14]. As demonstrated in ref. 15 it is possible to obtain a specific molecular arrangement avoiding the admixture of the ordered phases. In this way, we have grown α-CoPc thin films with herringbone and brickstone-like structures onto graphene (Gr) and Au(111) substrates, respectively. A disorded α-CoPc thin film (CoPc/ITO sample) was also fabricated as reference to clarify the molecular dynamics independently of the stacking geometry. Combined

[a] *Istituto Officina dei Materiali, Consiglio Nazionale delle Ricerche, Trieste, Italy.*
[b] *Department of Physics, Chandigarh University, Chandigarh, India.*
[c] *Department of Physics, University of Johannesburg, Johannesburg, South Africa.*
[d] *Laboratory of Quantum Optics, University of Nova Gorica, Ajdovščina, Slovenia.*
[e] *Elettra - Sincrotrone Trieste S.C.p.A, Trieste, Italy.*
[f] *FORTH Institute of Electronic Structure and Laser Foundation for Research and Technology Hellas and University Of Crete, Hellas.*
Corresponding author, **E-mail: cristian.soncini@ifn.cnr.it*
† Technische Universität Dortmund, Experimentelle Physik VI, Dortmund, Germany.

Electronic Supplementary Information (ESI) available: Methods, Structural characterization of the films, PES-IPES spectra analysis, TAS in the ns time domain and α-CoPc crystal structures. See DOI: 10.1039/x0xx00000x

photoemission spectroscopy (PES)-inverse photoemission spectroscopy (IPES) spectra was used to determine the molecular orbitals involved in the excited state dynamics. The complementary use of the information gained through TAS and time-resolved PES (TR-PES) allowed us to reconstruct the CoPc de-excitation pathways over 7 ns. Within few hundreds of fs we observe both rapid decay to the ground state, due to the non-radiative relaxation of the singlet excited states, and the formation of triplet states by ultrafast intersystem crossing (ISC). To rationalize the ultrafast ISC (spin-forbidden character process), we suggest the possible direct contribution of the $Co3d_{z^2}$ orbital in enabling a rapid evolution between singlet and triplet configurations: acting as intermediate may obviate the need for an energetically unfavorable spin-flip. Furthermore, we found a direct dependence of the CT exciton decay times on the molecular stacking, going from a few ps (brickstone structure) to tens of ps (herringbone structure). We ascribe such difference to the different π-conjugation along the molecular stacking axis, favoring the CT exciton delocalization in the herringbone geometry.

2 Results

2.1 Energy level alignment of CoPc/Gr and CoPc/Au(111) samples

The details of the samples' growth and structural characterization are reported in the ESI (Methods and Section S1). Before studying the molecular dynamics of α-CoPc herringbone and brickstone-like structures, we clarified the molecular orbitals involved in the excited state dynamics by PES and IPES measurements. The combined PES-IPES spectra of the two samples (thickness of about 24±2 nm) are shown in Figure 1a. The peaks labelled b and a, below E_F, are assigned to the ligand highest occupied molecular orbital (HOMO) and HOMO-1, respectively[16-19]. The unoccupied states, probed by IPES, show two distinct peaks within 1.5 eV (above E_F), namely c and d. Several theoretical works on the CoPc empty states are reported in the literature[14,17,20-23]. However, most of the published calculations are performed on the isolated molecule approximation, even though solid aggregation induces changes in the electronic properties of the organic semiconductors[24,25]. The calculated CoPc electronic structure is very sensitive to the theoretical functional used to model the exchange-correlation interactions. As a consequence, the nature of the first empty state is found either as a_{1g} symmetry state (orbital of mostly $Co3d_{z^2}$ character mainly localized on the Co atom) or ligand character (lowest unoccupied molecular orbital – LUMO – mostly localized over the Pc macrocycle)[17,21]. Before further discussing, we emphasize that a definitive assignment of the unoccupied states is beyond the scope of this article. In the following, we briefly report experimental works from the literature as a guideline to draw out a possible assignment of the features in our IPES spectra. IPES measurements of CoPc films assign the LUMO to an empty state feature located at about 1.7 eV above E_F[26,27], an energy comparable to our peak d. Furthermore, Yoshida and co-workers, similarly to our peak c, observe a shoulder below the LUMO which is tentatively attributed to an unoccupied state originating from the $Co3d_{z^2}$ [26] (In our case we observe two distinct peaks because of the higher IPES energy resolution). Betti et al.[28] from linear polarization XAS of the Co L_{23} edge of a CoPc/Au(110) thin film, assign the first resonance peak to the $Co3d_{z^2}$ orbital and the second one to Co3d orbitals with e_g symmetry (Co orbitals mixed in the LUMO states), confirming the assignment proposed by Yoshida and co-workers. Accordingly, as suggested by the reported literature, strictly by definition the LUMO should be defined as the a_{1g} symmetry state mainly originating from the $Co3d_{z^2}$ orbital. However, in the literature the LUMO is related to the final state of the CoPc optical transitions located at 1.8-2 eV in linear absorption spectra[12] (π-π* transitions localized on ligand-character orbitals)[§]. Therefore, to be consistent with the existing literature, in the following the LUMO is intended as the ligand-based e_g symmetry state involved in the optical absorption spectra.

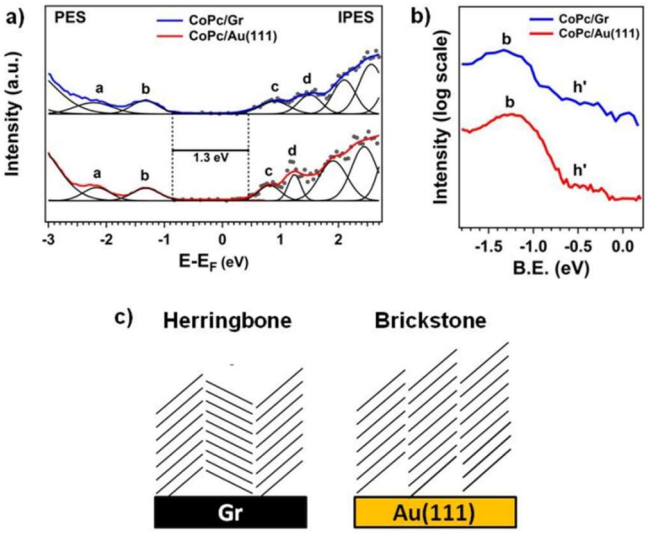

Figure 1. a) Combined PES-IPES spectra of the CoPc/Gr and CoPc/Au(111) samples. The evaluation of the energy level position of the peaks a, b, c and d is discussed in section S2 of the ESI; **b)** PES spectra of the CoPc/Gr and CoPc/Au(111) samples in the energy region close to E_F in logarithmic scale; **c)** sketch of the CoPc herringbone and brickstone structures.

Sample	Peak a	Peak b	Peak c	Peak d	b-d energy gap (HOMO-LUMO)	b-c energy gap (HOMO-$Co3d_{z^2}$)
CoPc/Gr	-2.20 eV	-1.30 eV	0.90 eV	1.50 eV	2.00 eV	1.30 eV
CoPc/Au(111)	-2.15 eV	-1.30 eV	0.85 eV	1.35 eV	1.85 eV	1.30 eV

Table 1. Summary of the peaks a, b, c and d in the two samples and the estimated b-d and b-c energy gaps obtained by linear extrapolation of the PES and IPES data (see ESI section S2).

Table 1 summarizes the binding energies and energy differences between filled and empty states estimated from the combined PES-IPES spectra. Considering that the CoPc HOMO-LUMO optical gap is 1.65 eV[‡], the peak d is compatible with the ligand LUMO (it shows an energy separation from the HOMO of about 1.9-2 eV). We recall that the transport gap measured by combined PES-IPES spectra which differs from the optical gap by the exciton binding energy. Therefore, similarly to previous reports of CoPc films in the literature[26-28], the peak c is compatible with the a_{1g} symmetry state originating from the unoccupied part of the $Co3d_{z^2}$ orbital. The

presence of additional states with Co3d character in the HOMO-LUMO gap is supported by DFT calculations based on the β-CoPc crystal phase[23].

As shown in Figure 1b, a shoulder of the ligand HOMO at about -0.5 eV, labelled h', is observed. As discussed in the ESI (Section S3), broadening of the HOMO induced by radiation damage can be safely excluded. Previous STM measurements[31] and VB spectra of CoPc thin films[16,18,32] point out the presence of a low-lying state to the HOMO and assigned it to the a_{1g} symmetry state originating from the occupied part of the $Co3d_{z^2}$ orbital.

It is worth noting that even though the screening effect could have a significant impact on the charge injection/extraction barrier at the metal/organic interface and gap evaluation of organic films deposited on metal surfaces (Au(111) in our case), its effect results strongly decreased at a thickness of about 10 nm[33]. For this reason, we ascribe the difference in the electronic properties detected in the two films (Table 1) to the different molecular arrangements.

2.2 Relaxation kinetics of α-CoPc films

Before discussing the excited state dynamics in the CoPc films, for the sake of clarity, the CoPc optical properties are briefly reported. The UV/Vis absorption of CoPc shows two bands, the Q band ($S_0 \rightarrow S_1$ transition), ranging between 1.7 eV-2.4 eV, and the Soret band ($S_0 \rightarrow S_2$ transition) at 3.7 eV, both involving π-π* excitations localized on the macrocycle[34-36]. The Q band is split into two components located at about 1.8 eV and 2 eV. The presence of a transition metal with half-filled d shell origins an additional component in the high-energy side of the Q band, the CT states (about 2.2 eV)[12,37,38]. Inter-molecular CT states are often coupled with intra-molecular exciton states gaining an appreciable intensity in the optical absorption spectra from excitation of the S_1 states[39,40 and refs therein].

The disordered CoPc/ITO film was first studied as a reference to point out the CoPc relaxation dynamics independently of the influence of molecular ordering. Figure 2a shows the TAS spectra obtained by using three different pump pulse energies, 3.1 eV (Soret band excitation, S_2), 2.41 eV (Q band excitation, S_1) and 1.21 eV (excitation into the CoPc HOMO-LUMO gap) at 0.25 ps and after 15 ps. Independently of the pump energy, all spectra in the Q band region show the same ESA features, namely I, II and III. The negative ESA signals I and III are assigned to the ground state bleaching due to the population of singlet excited states after the pump excitation[12]. The positive signal II is the induced absorption of triplet states ($T_1 \rightarrow T_2$) originated, through ISC from the singlet excited states after excitation ($S_1 \rightarrow T_1$)[12]. The decay times of the ESA features, obtained by fit (eq. S2), are summarized in Table 2. All three pumps show the same kinds of decay times. The kinetics of the ground state bleaching signals require to be modelled by a double exponential function, the signature of two distinct de-excitation pathways of the singlet states (decay times τ_1 and τ_2). However, the complete decay is not achieved within 15 ps. A residual bleaching signal is detectable over the ns time domain (ESI Figure S4), suggesting the need for an additional relaxation channel to fully restore the ground state. An additional feature at about 1.3 eV, marked H', is observed by using 3.1 eV and 1.21 eV pump pulses¶. Noteworthy, exciting the system with 1.21 eV (an energy comparable to the HOMO-$Co3d_{z^2}$ (unoccupied) energy separation in the combined PES-IPES spectra), H' becomes the dominant ESA feature. We will show that the dynamical process associated with H' may specifically involve the $Co3d_{z^2}$ orbital.

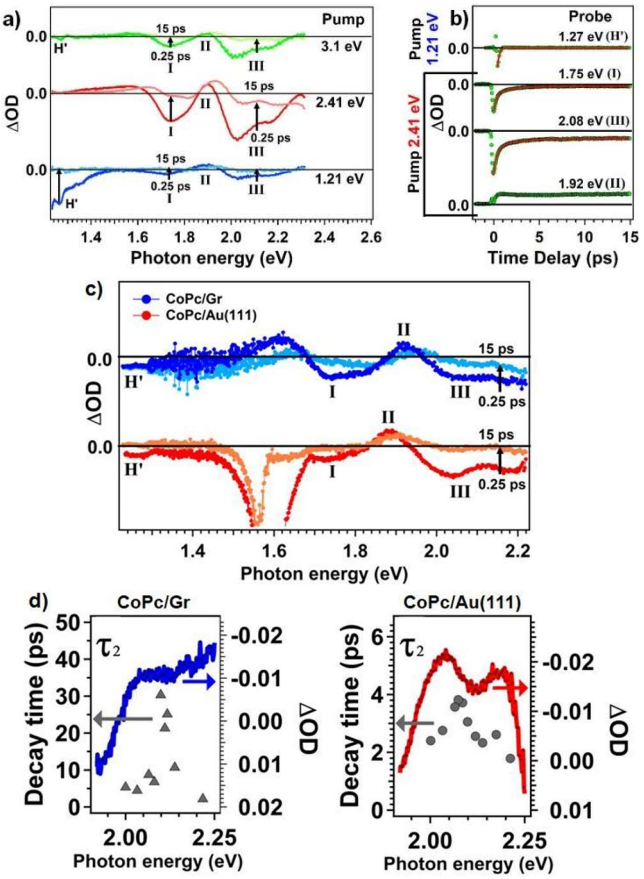

Figure 2. a) TAS spectra in transmittance mode of the CoPc/ITO sample using three different pump pulse energies; **b)** CoPc/ITO decay curves of the transient bands I, II and III using a 2.41 eV pump pulse and of H' using a 1.21 eV pump pulse; **c)** CoPc/Gr and CoPc/Au(111) TAS spectra in the Q band energy region; **d)** CoPc/Gr and CoPc/Au(111) decay time τ_2 (assigned to CT exciton kinetics) as a function of the probe photon energy. The bleaching signal III of both samples (blue and red curves) from TAS spectra are shown for comparison to highlight the energy position of the decay times within the transient band.

Sample	Probe photon energy			
	1.27 eV (H')	1.75 eV (I)	2.1 eV (III)	1.92 eV (II)
CoPc/ITO (disordered)	τ= 206 fs	τ_1= 285 fs τ_2= 1.78 ps	τ_1= 422 fs τ_2= 2.92 ps	τ= ns
CoPc/Au(111) (brickstone)	τ= 248 fs	τ_1= 292 fs τ_2= 1.56 ps	τ_1= 430 fs τ_2= 3.98 ps	τ= ns
CoPc/Gr (herringbone)	τ= ns	τ_1= 305 fs τ_2= 2.45 ps	τ_1= 408 fs τ_2= 20-30 ps	τ= ns

Table 2. Decay times of the CoPc samples (estimated by using eq. S2, see ESI section Methods) as a function of the probe photon energy.

The TAS spectra (2.41 eV pump) of the ordered CoPc/Gr and CoPc/Au(111) films are shown in Figure 2c. Both show TAS spectral features qualitatively identical to those of the

CoPc/ITO thin film, showing the ESA signals I, II, III and H' (the origin of I, II, and III has been previously discussed). The decay times obtained by fit (ESI eq. S2) are summarized in Table 2. In the ordered films, the decay time of H' is substantially different: sub-ps in the CoPc/Au(111) sample (similarly to the CoPc/ITO case) and ns in the CoPc/Gr sample. As discussed in the ESI Section S5, the ESA signal H' in the CoPc/Gr sample is due to a long-living dynamic of the Gr substrates i.e. not to the molecular film as in the other samples. Similarly, the intense ESA feature at 1.6 eV in the CoPc/Au(111) sample is a dynamic process of the Au(111) substrate. Due to the opaque substrates, TAS measurements were performed in reflection mode i.e. we were also sensitive to the kinetics of the substrates.

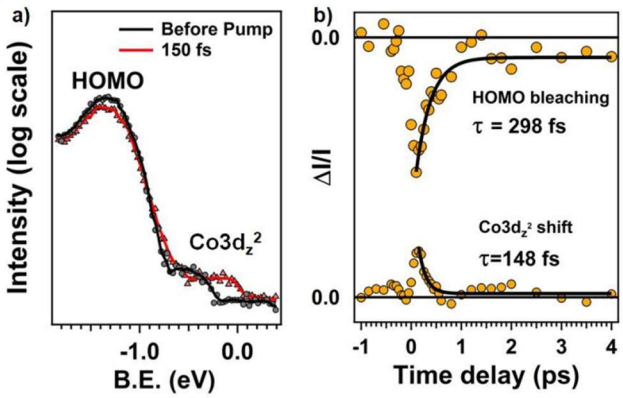

Figure 3. a) CoPc/Au(111) sample TR-PES spectra before and after the pump pulse; **b)** decay curve of the HOMO repopulation, ΔI is defined as the difference between the PES intensity with and without (I) the excitation pulse.

As shown in Table 2, the decay time τ_1 of the ground state bleaching signals is independent of the molecular structure, showing almost identical values in all three samples. This is a first suggestion of a relaxation process with intra-molecular character. On the contrary, at about 2.1 eV of photon energy, the decay time τ_2 shows a clear dependence on the CoPc structure (Figure 2d), going from 4 ps (brickstone structure) to tens of ps (herringbone structure). Noteworthy, this photon energy closely matches the energy region of the CT exciton component in the optical absorption spectra. Previous TAS measurements of a CoPc/quartz film in the literature, similarly to our case, report a relaxation dynamic centred at 2.04 eV assigned to the presence of a delocalized CT exciton band[12]. However, even though CT states are located in the high-energy side of the Q band, we observe CT exciton kinetics (decay time τ_2) over the whole Q band (ESA features I and III). This fact can be rationalized by taking into account the hybridization effects between CT and S_1 states. The degree of mixing between states is strongly related to their energy separation[39]. Due to the small energy difference between S_1 states of the LUMO (0.2 eV), a partial CT character is expected over the whole Q band energy region (even though with a lower degree of mixing at the low-energy side).

Figure 3a shows the CoPc/Au(111) TR-PES spectra using a 2 eV pump pulse. After pump excitation two effects are observable, the HOMO bleaching, due to the promotion of electrons into the LUMO, and a shift in energy toward E_F of the Co3d$_z^2$ peak. The decay curves are shown in Figure 3b. The HOMO bleaching shows a decay time of 298 fs, a value comparable to τ_1 of the ground state bleaching signals in TAS spectra. While the decay time of the Co3d$_z^2$ peak shift (148 fs) is highly similar to the decay time of H' in the CoPc/ITO and CoPc/Au(111) TAS spectra (Table 2).

3 Discussion

The complementary use of the information gained by TAS and TR-PES allowed us to reconstruct the CoPc de-excitation pathways up to 7 ns. A sketch of all the possible relaxation kinetics after excitation is shown in Figure 4. Firstly, the comparison between the TAS spectra of the CoPc/ITO sample (2.41 eV and 3.1 eV excitation energy) allows us to rule out the contribution of ultrafast intra-band (vibrational cooling) and inter-band relaxation processes (if detectable with TAS, they are faster than 250 fs). Exciting the system to S_2 or S_1, the ESA features are qualitatively identical (Figure 1a). In other words, the initial ultrafast relaxation (τ_1) in the Q band energy region is not due to the vibrational cooling (Kasha's rule predicts that it should be the first relaxation process to occur). Secondly, we observe the development of triplet states (ESA feature II) within 250 fs, suggesting that ISC from singlet to triplet states is faster and not assignable to the initial ultrafast relaxation (τ_1) of the ESA features I and III.

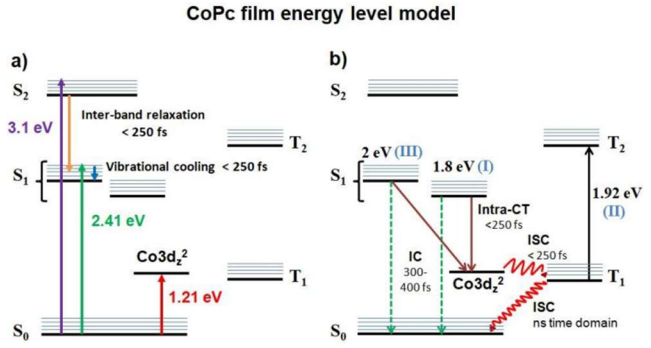

Figure 4. Energy level model of the CoPc in solid state describing the **a)** excitation in the molecular film using 1.21 eV, 2.41 eV and 3.1 eV pump pulses and the ultrafast inter-band and intra-band (vibrational cooling) relaxation processes; **b)** relaxation pathways in the CoPc film related to the ESA features observed in TAS spectra. The ESA feature II ($T_1 \rightarrow T_2$ transition) is observable only after the generation of triplet states.

As previously mentioned, the HOMO bleaching in TR-PES spectra has a decay time (repopulation of the HOMO from excited states) comparable to the τ_1 values of the ground state bleaching signals in TAS spectra (Figure 3a). Considering the lack of fluorescence of the CoPc[40,41] and that the de-excitation of triplet states occurs in the ns time domain (ESI Figure S4), we assign τ_1 to the non-radiative relaxation from S_1 to the ground state by internal conversion ($S_1 \rightarrow S_0$). Despite the spin-forbidden character of the ISC process, several studies in the literature, similarly to our case, report ultrafast ISC kinetics in transition metal phthalocyanines (MPcs) and porphyrins[12,13,42-44]. This behaviour has been rationalized supposing that the coupling between the metal 3d orbitals and the phthalocyanine-based exciton states provides additional

channels for the relaxation of the excited states, leading to high ISC quantum yield[42-44,45]. The substantial impact of the 3d orbitals in the molecular dynamics can be understood simply by comparing our CoPc TAS spectra with those of the CuPc film of ref. 13 (we recall that in the CuPc the single-occupied metal orbital is the $3d_{x^2-y^2}$ - in-plane oriented). The singlet excited states (S_1) of the CuPc decay in hundreds of ps (in the CoPc we observe an initial fast relaxation of a few ps). Furthermore, the CoPc spectra show an additional ESA feature (II) directly related to the formation of triplet states (not observed in the CuPc TAS spectra). Such differences highlight a possible important role of the $Co3d_{z^2}$ orbital in modifying as well as providing additional relaxation channels to the excited states. Our data suggest a possible direct contribution of the $Co3d_{z^2}$ orbital in enabling the ultrafast evolution between singlet and triplet configurations without involving spin-orbit coupling. In TR-PES spectra, although we selectively excite the S_1 states (2 eV pump pulse), a shift of the $Co3d_{z^2}$ peak toward E_F is also induced (Figure 3a). We hypothesize that a partial redistribution of the charge density between different atomic sites of the molecule would result in an energy shift of the $Co3d_{z^2}$ peak[46]. The promotion of an electron from the macrocycle to the single-occupied $Co3d_{z^2}$ orbital (intra-molecular CT process) would lead to its complete occupancy and charge redistribution toward the Co atomic site. We recall that the HOMO has mainly atomic orbital contribution from the C atoms of the macrocycle and the $Co3d_{z^2}$ orbital is localized on the Co atom[17,18,32]. Such electron transfer changes the CoPc electronic configuration from $^2A_{1g}$ to $^2A_{1u}$ (high-energy configuration of about 0.2 eV)[22]. Ha-Thi and co-workers show that CT states (involving half-filled metal 3d orbitals) acting as intermediate ($^2S \rightarrow {}^2CT \rightarrow {}^2T$), may obviate the need for an unfavourable spin-orbit coupling enabling the rapid evolution between singlet and triplet configurations[42]. We invoke a similar mechanism, hypothesizing that the ultrafast generation of triplet states is a consequence of electron exchange between phthalocyanine S_1 states and the $Co3d_{z^2}$ orbital. After electron pairing in the $Co3d_{z^2}$ ($^2S_1 \rightarrow {}^2CT$), an electron with opposite spin (with respect to the received) is returned generating the T_1 state ($^2CT \rightarrow {}^2T_1$). This return is driven by the indiscernibility of paired electrons and the energy minimization of the T state as compared to the S state. This mechanism seems reasonable considering that T states are usually located at about half-energy of the S states, being in this case, energetically close to the $Co3d_{z^2}$ orbital. Furthermore, we note that de-excitation through T states is one of the main relaxation channels of S_1 states in CoPc thin films. As shown in Figures 2a-c, after an initial partial relaxation through IC, a long-lasting bleaching signal of the S_1 states persists over the ns time domain (ESI Figure S4). Similarly, the ESA signal of the T_1 states is almost constant over 7 ns (ESI Figure S4). This fact suggests that no further relaxation of S_1 states occurs as long as the T_1 states decays to the ground state.

Finally, our data show that the kinetics of the CT exciton (τ_2) in CoPc films depends on the molecular arrangement, leading to an enhanced lifetime in the herringbone case (Figure 2d). The decay kinetics of CT excitons in anisotropic π-conjugated systems is modelled by two rate constants, which consider the intrinsic exciton lifetime and the decay rate through the exciton-exciton annihilation mechanism[47,48]. The higher the concentration of CT excitons, the more the recombination by the CT bi-exciton annihilation process is relevant. In our case considering the excitation density of 10^{21} cm^{-3}, both recombination mechanisms are expected in determining the CT exciton lifetime. The interplay between CT exciton transfer (hopping) to neighbour molecular sites and the annihilation radius (generally approximated by the distance between donor-acceptor pairs) determines the mobility of CT excitons [48,49]. Delocalizing the charge of CT excitons reduces the Coulomb attraction of CT states and the probability of charge recombination[49]. In other words, a more efficient delocalization (higher hopping rate) due to a more favourable orbital overlap between adjacent molecules leads to an enhanced CT exciton lifetime.

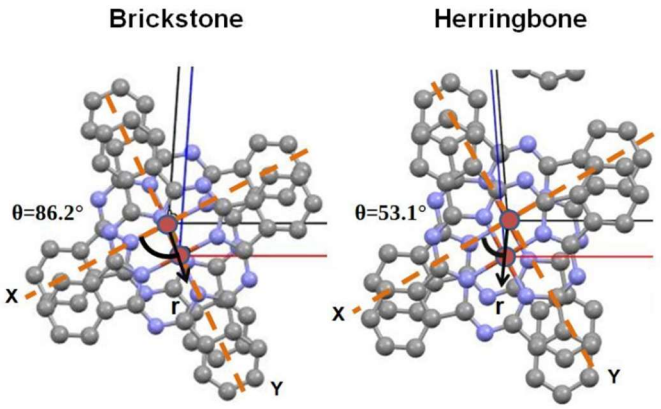

Figure 5. Two neighbouring CoPc molecules in the brickstone and herringbone structures (top view) illustrate the different sliding angle in the two cases. The atoms are colour coded, i.e., Co is in red, C is in grey and N is in blue. The sliding angle is labelled θ. The vector r and the X and Y axes are used to define the sliding angle.

Lattice parameter	CoPc	
	brickstone[50]	herringbone[51]
Co-Co distance (Å)	3.75(4)	3.75(0)
Inter-plane distance (Å)	3.42(5)	3.40(6)
Edge-to-edge distance (Å)	3.5-4	3.5-4
Stacking angle (°)	65.8	65.3
Sliding angle (°)	86.2	53.1

Table 3. Summary of the brickstone and herringbone lattice parameters reported from literature[50,51]. For further details see ESI section S6.

As a consequence, the crystal structure plays a key role in the CT exciton kinetics, possibly explaining the enhanced lifetime observed in the herringbone stacking. In highly anisotropic crystals it is unlikely to assume isotropic CT diffusion, so hopping along a preferential axis is a more realistic description. Considering the significant π-π interaction along the CoPc stacking axis, CT exciton energy transfer is expected to be fastest along this axis. Possible CT exciton delocalization through inter-stack axes may also be present. However, their

contributions should be substantially lower (significantly lower orbital overlap). Table 3 summarizes the lattice parameters of the herringbone and brickstone structures of α-CoPc crystals reported from literature[50-51]. The edge-to-edge distances (inter-stack distance along the axes perpendicular to the molecular stacking) are comparable, suggesting that the difference in CT exciton kinetics most likely originates along the stacking axis. However, the almost identical inter-plane distances (assumed as the annihilation radius), Co-Co distances and stacking angles suggest comparable annihilation rates and metal orbital coupling along the stacking axis. Nevertheless, the significant difference in the sliding angle could be the origin of the different CT exciton kinetics (Figure 5). A different sliding angle may induce differences in the orbital overlap between adjacent molecules along the stack. In highly conjugated π-systems, an increased intermolecular overlap of electronic wave functions leads to increased bandwidth, which is directly related to charge transport[52]. We hypothesize that due to a higher π-wavefunction overlap in the herringbone stacking geometry, the CT exciton is delocalized more efficiently along the stacking axis, enhancing its lifetime.

4 Conclusions

In summary, CoPc films with different structural arrangements (disordered, herringbone and brickstone) were fabricated and the influence of the different intermolecular interactions on the CT dynamical properties was evaluated. A detailed characterization of the electronic and dynamical properties of the CoPc thin films was obtained by using a muti-technique approach. Combined PES-IPES clarified the molecular orbitals involved in the excited state dynamics. The complementary use of the information gained by TAS and TR-PES allowed us to reconstruct the CoPc intra and inter-molecular de-excitation pathways up to 7 ns. We suggest that the ultrafast ISC (faster than 250 fs) observed in CoPc could be driven by an intermediate intra-molecular CT state, enabling a rapid evolution between singlet and triplet configurations. The mechanism involves the electron exchange between the $Co3d_{z^2}$ orbital and π orbitals of the macrocycle, avoiding an energetically unfavourable spin-flip. Finally, the CoPc film with herringbone structure shows enhanced CT exciton lifetime, demonstrating the active role of the molecular arrangement in modulating CT dynamics. We hypothesize a more efficient CT exciton delocalization due to a higher π-wavefunction overlap in the herringbone stacking geometry. This work highlights the significant role of the 3d metal orbitals in providing additional channels for energy transfer as well as that a fine-tuning of the molecular structure allows modulating CT processes at the nanoscale.

Author Contributions

C. Soncini, M. Pedio and A. Kumar conceived and planned the experiment, contributed to the growth of the samples and carried out the spectroscopic characterization (PES, IPES, TR-PES, XAS and TAS measurements). E. Magnano and F. Bondino performed XAS measurements, B. Ressel, M. Stupar and G. Di Ninno carried out PES and TR-PES measurements, A. Papadopoulos, E. Serpetzoglou and E. Stratakis performed TAS measurements. The manuscript was written through the contributions of all authors. All authors have approved the final version of the manuscript.

Conflicts of interest

There are no conflicts to declare.

Acknowledgements

Igor Pis is kindly acknowledged for his support during XAS measurements. Alessandra Matruglio and Marco Lazzarino are kindly acknowledged for providing the $Gr/SiO_2/Si$ substrates. This work is partially supported by the Elettra Proposal number 20210343. The CNR-IOM technical staff members, Stefano Bigaran, Federico Salvador, Paolo Bertoch, Davide Benedetti and Andrea Martin, are kindly acknowledged for their support.

Notes and references

§ We hypothesize that due to drastically different transition probabilities, in CoPc optical absorption spectra, the dominant transition is from the HOMO to ligand-based π-unoccupied orbitals (ligand LUMO) and the possible HOMO-a_{1g} optical transition is not observed. Even though the energy range of the HOMO-a_{1g} optical transition (about 1.3 eV) is not generally accessible with standard UV/Vis spectrometers.

‡ Calculated from the optical absorption spectra of ref. 12 by Tauc method[29,30].

¶ The lack of H' by using a 2.41 eV pump pulse may be due to its superimposition to the broad positive induced absorption signal ranging from 1.3 eV to 1.6 V (whose intensity is highly enhanced at this excitation energy).

1 H.Bronstein, C.B. Nielsen, B.C.Schroeder and I.McCulloch. The role of chemical design in the performance of organic semiconductors. *Nature Reviews Chemistry* **2020,** 4, 66–77.

2 M. Ding, X. Gu, L. Guo, R. Zhang, X. Zhu, R. Li, X. Zhang, W. Hua and X. Sun. The prospects of organic semiconductor single crystals for spintronic applications. *J. Mater. Chem. C* **2022**, 10, 2507–2515.

3 C. Qian, J. Sun, and Y. Gao. Transport of charge carriers and optoelectronic applications of highly ordered metal phthalocyanine heterojunction thin films. *Phys. Chem. Chem. Phys.* **2021**, 23, 9631.

4 V. Coropceanu, J. Cornil, D. A. da Silva Filho, Y. Olivier, R. Silbey and J.-L. Bredas. Charge transport in organic semiconductors. *Chem. Rev.* **2007**, 107, 926-952.

5 D. Shen, Y. Wu, M.-F. Lo and C.-S. Lee. Charge transport properties of co-evaporated organic–inorganic thin film charge transfer complexes: effects of intermolecular interactions. *J. Mater. Chem. C* **2020**, 8, 16725.

6 J. Zhu, H. Hayashi, M. Chen, C. Xiao, K. Matsuo, N. Aratani, L. Zhang and H. Yamada. Single crystal field-effect transistor of tetrabenzoporphyrin with a one-dimensionally extended columnar packing motif exhibiting efficient charge transport properties. *J. Mater. Chem. C* **2022**, 10, 2527.

7 H. Lim, S. Yang, S.-H. Lee, J.-Y. Lee, Y. Lee, A. B. Situmorang, Y.-H. Kim, and J. W. Kim. Influence of the metal phthalocyanine molecular orientation on charge separation

at the organic donor/acceptor interface. *J. Mater. Chem. C* **2021**, 9, 2156.
8 C. Videlot, A. El Kassmi, and D. Fichou. Photovoltaic properties of octithiophene-based Schottky and p/n junction Cells: Influence of molecular orientation. *Sol. Energy Mater. Sol. Cells* **2000**, 63, 69-82.
9 S. Duhm, G. Heimel, I. Salzmann, H. Glowatzki, R. L. Johnson, A. Vollmer, J. P. Rabe, and N. Koch. Orientation-dependent ionization energies and interface dipoles in ordered molecular assemblies. *Nat. Mater.* **2008**, 7, 326.
10 L. Yu, Y. Hu, J. Li, Z. Wang, H. Zhang, Y. Huang, Y. Lou, Y. Sun, X. Lu, H. Liu, Y. Zheng, S. Wang, X. Chen, D. Ji, L. Li and W. Hu. High mobility n-type organic semiconductors with tunable exciton dynamics toward photo-stable and photo-sensitive transistors. *J. Mater. Chem. C* **2022**, 10, 8874.
11 K. Ozawa, S. Yamamoto, T. Miyazawa, K. Yano, K. Okudaira, K. Mase and I. Matsuda. Influence of Stacking Order of Phthalocyanine and Fullerene Layers on the Photoexcited Carrier Dynamics in Model Organic Solar Cell. *J. Phys. Chem. C* **2021**, 125, 13963−13970.
12 A. Gadalla, J. B. Beaufrand, M, Bowen, S. Boukari, E. Beaurepaire, O. Crégut, M. Gallart, B. Honerlage, and P. Gilliot. Ultrafast Optical Dynamics of Metal-Free and Cobalt Phthalocyanine Thin Films II: Study of Excited-State Dynamics. *J. Phys. Chem. C* **2010**, 114, 17854–17863.
13 B. W. Caplins, T. K. Mullenbach, R. J. Holmes, and D. A. Blank. Femtosecond to nanosecond excited state dynamics of vapor deposited copper phthalocyanine thin films. *Phys. Chem. Chem. Phys.* **2016**, 18, 11454.
14 W. Wu, N.M. Harrison and A. J. Fisher. Electronic structure and exchange interactions in cobalt-phthalocyanine chains. *Phys. Rev. B* **2013**, 88, 024426.
15 A. C. Cruickshank, C. J. Dotzler, S. Din, S. Heutz, M. F. Toney and M. P. Ryan. The Crystalline Structure of Copper Phthalocyanine Films on ZnO(1-100). *J. Am. Chem. Soc.* **2012**, 134, 14302−14305.
16 P. Gargiani, M. Angelucci, C. Mariani and M. G. Betti. Metal-phthalocyanine chains on the Au(110) surface: Interaction states versus d-metal states occupancy. *Phys. Rev. B* **2010**, 81, 085412.
17 E. Salomon, P. Amsalem, N. Marom, M. Vondracek, L. Kronik, N. Koch and T. Angot. Electronic structure of CoPc adsorbed on Ag(100): Evidence for molecule-substrate interaction mediated by Co 3d orbitals. *Phys. Rev. B* **2013**, 87, 075407.
18 V. V. Maslyuk, V. Y. Aristov, O. V. Molodtsova, D. V. Vyalikh, V.M. Zhilin, Y.A. Ossipyan, T. Bredow, I. Mertig and M. Knupfer. The electronic structure of cobalt phthalocyanine. *Applied Physics A* **2009**, 94, 485-489.
19 T. Zhang, I. E. Brumboiu, V. Lanzilotto, J. Lüder, C. Grazioli, E. Giangrisostomi, R. Ovsyannikov, Y. Sassa, I. Bidermane, M. Stupar, M. de Simone, M. Coreno, B. Ressel, M. Pedio, P. Rudolf, B. Brena and C. Puglia. Conclusively Addressing the CoPc Electronic Structure: A Joint GasPhase and Solid-State Photoemission and Absorption Spectroscopy Study. *J. Phys. Chem. C* **2017**, 121, 26372−26378
20 N. Marom and L. Kronik. Density functional theory of transition metal phthalocyanines, I: electronic structure of NiPc and CoPc—self-interaction effects. *Appl. Phys.* A **2009**, 95, 159–163
21 I. Emilia Brumboiu, G. Prokopiou, L. Kronik, and B. Brena. Valence electronic structure of cobalt phthalocyanine from an optimally tuned range-separated hybrid functional. *J. Chem. Phys.* **2017**, 147, 044301.
22 M.-S. Liao and S. Scheiner. Electronic structure and bonding in metal phthalocyanines, Metal=Fe, Co, Ni, Cu, Zn, Mg. *J. Chem. Phys*. **2001**, 114, 8.
23 H. A. R. Aliabad and M. Bashi. Cobalt phthalocyanine polymer for optoelectronic and thermoelectric applications. *Journal of Material Science: Materials in Electronics* **2019**, 30, 18720–18728.
24 L. Kronik and J. B. Neaton. Excited-State Properties of Molecular Solids from First Principles. Annual Review of Physical Chemistry **2016**, 67, 587-616.
25 M. Marsili, P. Umari, G. Di Santo, M. Caputo, M. Panighel, A. Goldoni, M. Kumar and M. Pedio. Solid state effects on the electronic structure of H2OEP. Phys. Chem. Chem. Phys. **2014**, 16, 27104-11 .
26 H. Yoshida, K. Tsutsumi and N. Sato. Unoccupied electronic states of 3d-transition metal phthalocyanines (MPc: Mn, Fe, Co, Ni, Cu and Zn) studied by inverse photoemission spectroscopy. *Journal of Electron Spectroscopy and Related Phenomena* **2001**, 121, 83–91.
27 J. Xiao and P. A. Dowben. The role of the interface in the electronic structure of adsorbed metal(II) (Co, Ni, Cu) phthalocyanines. *J. Mater. Chem.* **2009**, 19, 2172–2178.
28 M. G. Betti, P. Gargiani, R. Frisenda, R. Biagi, A. Cossaro, A. Verdini, L. Floreano and C. Mariani. Localized and Dispersive Electronic States at Ordered FePc and CoPc Chains on Au(110). *J. Phys. Chem. C* **2010**, 114, 21638–21644.
29 J. Tauc, R. Grigorovici, and A. Vancu. Optical Properties and Electronic Structure of Amorphous Germanium. *Phys. Status Solidi B* **1966**, 15, 627−637.
30 N. F. Mott, and E. A. Davis. Electronic Processes in Non-Crystalline Materials. *OUP Oxford* **2012**.
31 D. E. Barlow, L. Scuderio and K. W. Hipps. Scanning Tunneling Microscopy Study of the Structure and Orbital-Mediated Tunneling Spectra of Cobalt(II) Phthalocyanine and Cobalt(II) Tetraphenylporphyrin on Au(111): Mixed Composition Films. *Langmuir* **2004**, 20, 4413.
32 M. Grobosch, V. Yu. Aristov, O. V. Molodtsova, C. Schmidt, B. P. Doyle, S. Nannarone and M. Knupfer. Engineering of the Energy Level Alignment at Organic Semiconductor Interfaces by Intramolecular Degrees of Freedom: Transition Metal Phthalocyanines. *J. Phys. Chem. C* **2009**, 113, 13219–13222.
33 T. Aihara, S. A. Abd-Rahman and H. Yoshida. Metal screening effect on energy levels at metal/organic interface: Precise determination of screening energy using photoelectron and inverse-photoelectron spectroscopies. Phys. Rev. B **2021**, 104, 085305 .
34 A. Davidson. The effect of the metal atom on the absorption spectra of phthalocyanine films. *J. Chem. Phys.* **1982**, 77, 168.
35 H. Höchst, A. Goldmann, S. Hüfner, and H. Malter. X-Ray Photoelectron Valence Band Studies on Phthalocyanine Compounds. *Phys. Status Solidi B* **1976**, 76, 559.
36 M. M. El-Nahass, Z. El-Gohary and H.S. Soliman. Structural and optical studies of thermally evaporated CoPc thin films. *Opt. Laser Technol.* **2003**, 35, 523.
37 M. Knupfer, T. Schwieger, H. Peisert and J. Fink. Mixing of Frenkel and charge transfer excitons in quasi-one-dimensional copper phthalocyanine molecular crystals. *Phys. Rev. B* **2004**, 69, 165210.
38 H. Yoshida, Y. Tokura and T. Koda. Charge-transfer excitation bands in electro-absorption spectra of metal (Co, Ni, Cu, Zn)-phthalocyanine films. *Chemical Physics* **1986**, 109, 375-382.
39 J. P. Hernandez and S. I. Choi. Optical Absorption by Charge-Transfer Excitons in Linear Molecular Crystals. *J. Chem. Phys.* **1969**, 50, 1524.
40 H. Isago. Optical Spectra of Phthalocyanines and Related Compounds. *Springer: Tokyo* **2015**.
41 P. S. Vincett, E. M. Voigt, and K. E. Rieckhoff. Phosphorescence and Fluorescence of Phthalocyanines. *J. Chem. Phys.* **1971**, 55, 8.
42 M.-H. Ha-Thi, N. Shafizadeh, L. Poisson and B. Soep. An Efficient Indirect Mechanism for the Ultrafast Intersystem

Crossing in Copper Porphyrins. *J. Phys. Chem. A* **2013**, 117, 8111−8118.

43 G. J. Dutton, W. Jin, J. E. Reutt-Robey and S. W. Robey. Ultrafast charge-transfer processes at an oriented phthalocyanine/C_{60} interface. *Phys. Rev. B: Condens. Matter Mater. Phys.* **2010**, 82, 073407.

44 Y. Yan, S. Lu, R. Zhu, J. Zhou, S. Wei, and S. Qian. Ultrafast Excited State Dynamics of Modified Phthalocyanines: p-HPcZn and p-HPcCo*. J. Phys. Chem. A* **2006**, 110, 10757.

45 A. Antipas, and M. Gouterman. Electronic States of Co, Ni, Rh, and Pd Complexes. *J. Am. Chem. Soc.* **1983**, 105, 4896.

46 E. Wruss, G. Prokopiou, L. Kronik, E. Zojer, O. T. Hofmann and D. A. Egger. Magnetic configurations of open-shell molecules on metals: The case of CuPc and CoPc on silver. *Phys. Rev. Mat.* **2019**, 3, 086002.

47 R. J. Hudson, D. M. Huang and T. W. Kee. Anisotropic Triplet exciton diffusion in crystalline functionalized pentacene. *J. Phys. Chem. C* **2020**, 124, 23541−23550.

48 M. S. Myong, Y. Qi, C. Stern and M. R. Wasielewski. Ultrafast photo-driven charge transfer exciton dynamics in mixed-stack pyrene-perylenediimide single co-crystals. *J. Mater. Chem. C*, **2021**, 9, 16911.

49 G. Zhang, X. K. Chen, J. Xiao, P. Chow, M. Ren, G. Kupgan, X. Jiao, C. Chan, X. Du, R. Xia, Z. Chen, J. Yuan, Y. Zhang, S. Zhang, Y. Liu, Y. Zou, H. Yan, K. S. Wong, V. Coropceanu, N. Li, C. J. Brabec, J. L. Bredas, H. L. Yip and Y. Cao. Delocalization of exciton and electron wavefunction in non-fullerene acceptor molecules enables efficient organic solar cells. *Nat. Commun.* **2020**, 11, 3943.

50 P. Ballirano, R. Caminiti, C. Ercolani, A. Maras and M. A. Orrù. X-ray Powder Diffraction Structure Reinvestigation of the R and â Forms of Cobalt Phthalocyanine and Kinetics of the α→β Phase Transition. *J. Am. Chem. Soc.* **1998**, 120, 12798-12807

51 M. Ashida, N. Uyeda and E. Suito. Unit cell metastable-form constants of various phthalocyanine. *Bull. Chem. Soc. Jpn.* **1966**, 39, 2616.

52 a) H. Klauk. Organic Electronics Materials, Manufacturing and Applications. Wiley-VCH, Weinheim, **2006**; b) C. D. Dimitrakopoulos and P. R. L. Malenfant. Organic Thin Film Transistorsfor Large Area Electronics. *Adv. Mater.* **2002**, 14, 99; c) C. Reese, M. Roberts, M.-M. Ling and Z. Bao. Organic thin film transistors. Mater. Today 2004, 7, 20.